Development 140, 1871-1881 (2013) doi:10.1242/dev.088435

The p21-activated kinase Mbt is a component of the apical protein complex in central brain neuroblasts and controls cell proliferation

Juliane Melzer[1,*], Karoline F. Kraft[2,*], Rolf Urbach[2,‡] and Thomas Raabe[1,‡]

SUMMARY

The final size of the central nervous system is determined by precisely controlled generation, proliferation and death of neural stem cells. We show here that the *Drosophila* PAK protein Mushroom bodies tiny (Mbt) is expressed in central brain progenitor cells (neuroblasts) and becomes enriched to the apical cortex of neuroblasts in a cell cycle- and Cdc42-dependent manner. Using mushroom body neuroblasts as a model system, we demonstrate that in the absence of Mbt function, neuroblasts and their progeny are correctly specified and are able to generate different neuron subclasses as in the wild type, but are impaired in their proliferation activity throughout development. In general, loss of Mbt function does not interfere with establishment or maintenance of cell polarity, orientation of the mitotic spindle and organization of the actin or tubulin cytoskeleton in central brain neuroblasts. However, we show that *mbt* mutant neuroblasts are significantly reduced in cell size during different stages of development, which is most pronounced for mushroom body neuroblasts. This phenotype correlates with reduced mitotic activity throughout development. Additionally, postembryonic neuroblasts are lost prematurely owing to apoptosis. Yet, preventing apoptosis did not rescue the loss of neurons seen in the adult mushroom body of *mbt* mutants. From these results, we conclude that Mbt is part of a regulatory network that is required for neuroblast growth and thereby allows proper proliferation of neuroblasts throughout development.

KEY WORDS: Neuroblast, PAK, Mushroom body

INTRODUCTION

The central nervous system (CNS) in *Drosophila* arises from neuronal progenitor cells (neuroblasts), which are selected and specified during embryogenesis in a precise spatio-temporal order (Skeath and Thor, 2003; Urbach and Technau, 2004). Neuroblasts delaminate from the neuroectoderm and thereby inherit an apico-basal polarity axis. Along this axis, they divide asymmetrically in a stem cell-like mode to self-renew and generate a smaller, further differentiated ganglion mother cell (GMC), which divides only once to generate a pair of neurons or glia cells. In mitotic neuroblasts, the Par protein complex, which consists of Bazooka, Par6 and atypical protein kinase C (aPKC), localizes at the apical cortex and controls the basal localization of cell fate determinants, the orientation of the mitotic spindle along the apico-basal axis and asymmetry of the mitotic spindle, in order to generate daughter cells with different sizes. The Par complex is linked via Inscuteable (Insc) to the Partner of Inscuteable (Pins) protein complex, which in turn controls spindle orientation and asymmetry. Basal proteins include the adaptor protein Miranda, its associated proteins Brain tumor (Brat) and Prospero (Pros), and the Partner of Numb (Pon)-Numb complex, which determine the fate of the GMC, restrict its proliferative potential and induce differentiation (reviewed by Chia et al., 2008; Doe, 2008; Wu et al., 2008; Knoblich, 2010).

Two phases of neurogenesis can be distinguished. Delaminated neuroblasts proliferate until the end of embryogenesis, when most neuroblasts cease to divide and enter quiescence, which is a dormant non-proliferative state (Truman and Bate, 1988). In early larvae, neuroblasts start to reactivate and by 48 hours after larval hatching (ALH) neuroblasts have resumed proliferation (Truman and Bate, 1988; Chell and Brand, 2010). Exit from quiescence, and thereby activation of proliferation, in early larvae depends on nutrition and is governed by insulin signaling (Britton and Edgar, 1998; Chell and Brand, 2010; Sousa-Nunes et al., 2011). Postembryonic neuroblasts generate most of the future adult CNS by proliferating until third instar or pupal stage, depending on the neuroblast lineage, and terminate proliferation by final differentiation or apoptosis (Ito and Hotta, 1992; Bello et al., 2003; Maurange et al., 2008; Siegrist et al., 2010). The neuroblasts that generate the mushroom body (MBNBs), a paired central brain neuropil that is important for olfactory learning and memory, show a different proliferation pattern as they proliferate until late pupal stage without entering quiescence (Ito and Hotta, 1992).

We have previously identified the p21-activated kinase (PAK) Mbt as a viable structural brain mutant (Melzig et al., 1998). PAK proteins are effectors of the RhoGTPases Rac and Cdc42. Owing to structural and regulatory differences, PAK proteins are classified into group I and group II PAKs. In *Drosophila*, PAK1 and PAK2 are group I representatives and Mbt is the single group II PAK. Different PAK proteins fulfill common and distinct functions in a variety of cellular processes that depend on selective binding of RhoGTPases and their upstream regulators, subcellular localization and other isoform-specific protein interactions (reviewed by Arias-Romero and Chernoff, 2008; Eswaran et al., 2008; Wells and Jones, 2010). PAK proteins play important roles in neurogenesis and maintenance of neuronal functions in different species (reviewed by Kreis and Barnier, 2009; Chan and Manser, 2012). The

[1]Universität Würzburg, Institut für Medizinische Strahlenkunde und Zellforschung, Versbacherstr. 5, D-97078 Würzburg, Germany. [2]Universität Mainz, Institut für Genetik, J.-J.-Becherweg 32, D-55099 Mainz, Germany.

*These authors contributed equally to this work
‡Authors for correspondence (urbach@uni-mainz.de; thomas.raabe@mail.uni-wuerzburg.de)

Accepted 20 February 2013

Drosophila group I PAK proteins have been reported to regulate different aspects of neural development, such as axonal guidance (reviewed by Kreis and Barnier, 2009) and synapse development (Parnas et al., 2001; Albin and Davis, 2004; Ozdowski et al., 2011). The group II PAK protein Mbt localizes at adherens junctions in the developing eye to control morphogenetic processes (Schneeberger and Raabe, 2003; Menzel et al., 2007). The phenotypic analysis of *mbt* mutants also indicated a requirement in CNS development either in generation or survival of neurons (Melzig et al., 1998). In this report, we verify that Mbt is enriched in a Cdc42-dependent manner at the apical cortex of larval brain neuroblasts during mitosis. Mutation of *mbt* does not interfere with basic features of asymmetric cell division or organization of the cytoskeleton. Using the well-defined MBNB lineages, we show that *mbt* mutant neuroblasts are specified correctly and in principle can generate the different types of mushroom body neurons. Mutant neuroblasts are characterized by their smaller cell size and their impairment in mitotic activity throughout development, which finally leads to premature cell death. We conclude that Mbt is required for normal neuroblast growth as an important prerequisite for proper proliferation.

MATERIALS AND METHODS

Fly stocks and culture

The following fly stocks were used: mbt^{P1} (Melzig et al., 1998), $Cdc42^{3}$ (Genova et al., 2000), *Df(3L)H99* [Bloomington Stock Center (BL) #1576], *Ubi-P-Myc::Cdc42* (Genova et al., 2000), *UAS-mbt*, *UAS-*$mbt^{H19,22L}$, *UAS-*mbt^{T525A}, *UAS-*mbt^{K397M} (Schneeberger and Raabe, 2003), *worniu-GAL4* (Albertson and Doe, 2003), *P{GawB}*ey^{OK107} (Bl#854) and *UAS-p35* (Bl#5072).

For MARCM analysis (Lee et al., 1999), mbt^{P1}, *FRT19A; P{GawB}*ey^{OK107}/+ flies were crossed with *hsFLP, tubP-GAL80, FRT19A; UAS-mCD8::GFP* (BL #5134). Wild type was w^{1118} in all experiments, except for the MARCM analysis, where $y^{1}w^{1118}$ *P{neoFRT}19A* (BL #1744) was used. All crosses were performed at 25°C except for the MARCM analysis. Those crosses were kept at 18°C after two consecutive heat-shocks for 1 hour at 37°C at first or third larval stage. Flies analyzed had the genotype *FRT19A/ hsFLP, tubP-GAL80, FRT19A; UAS-mCD8::GFP/+; P{GawB}*ey^{OK107}/+ or mbt^{P1}, *FRT19A/ hsFLP, tubP-GAL80, FRT19A; UAS-mCD8::GFP/+; P{GawB}*ey^{OK107}/+.

Larval staging

Newly hatched larvae were collected from apple juice plates at 30-minute intervals and transferred to standard fly food plates with yeast. Larvae were kept at 25°C until they reached the desired age. Larval stages were determined before preparation by means of spiracle morphology. Thirty-six-hour-old larvae were L2, 48 hour larvae and older were L3.

Immunostainings

Embryos were immunostained according to previously published protocols (Urbach et al., 2003). Larval brains were dissected in PBS and fixed on ice for 25 minutes in PLP solution (2% paraformaldehyde, 0.01 M $NaIO_4$, 0.075 M lysine, 0.03 M sodium-phosphate buffer pH 6.8). For anti-α-Tubulin staining, brains were fixed in 3.7% paraformaldehyde for 30 minutes at room temperature. All washings were carried out in PBT (PBS containing 0.3% Triton X-100). After blocking in 5% normal goat serum in PBT, brains were incubated with the following primary antibodies: mouse anti-Armadillo [1:100, Developmental Studies Hybridoma Bank (DSHB)], rabbit anti-β-Gal (1:2000, Promega), chicken anti-β-Gal (1:1000, Abcam), mouse anti-Dac (1:250, DSHB), rabbit anti-Dmef2 (1:750, H. T. Nguyen, Erlangen, Germany), guinea pig anti-Dpn (1:1000, J. Skeath, St Louis, MO, USA), rat anti-Elav (1:400, DSHB), rabbit anti-Ey (1:1000, U. Walldorf, Saarbrücken, Germany), rat anti-Ey (1:5000, P. Callaerts, Leuven, Belgium), mouse anti-FasII (1:10, DSHB), rabbit anti-GFP (1:1000, MoBiTec/Molecular Probes), rabbit anti-Mira (1:500, J. Knoblich, Vienna, Austria), mouse anti-Mir (1:20, F. Matsuzaki, Kobe, Japan), rabbit anti-Mbt (1:500) (Schneeberger and Raabe, 2003), mouse anti-Nrt (1:10, DSHB), guinea pig anti-Numb (1:1000, J. Skeath), mouse anti-PH3 (1:1000, Cell Signaling), rabbit anti-PH3 (1:2500, Millipore Upstate), rat anti-Pins (1:500, F. Matsuzaki), rabbit anti-PKCζ clone C20 (1:1000, Santa Cruz Biotechnology), mouse anti-Pros (1:100, DSHB), rabbit-anti-Tll (1:600, John Reinitz, New York, USA), mouse anti-γ-Tubulin (1:100, Sigma) and mouse anti-α-Tubulin (1:500, clone DM1A, Sigma). Secondary antibodies were AlexaFluor 488 (Molecular Probes), or Cy3, Cy5, Alexa 568, Alexa 647 and Dylite 549 conjugated (Dianova). F-actin was visualized with Phalloidin-Rhodamine (1:30, Sigma) or Phalloidin-Oregon Green (1:500, Invitrogen). After embedding in Vectashield, confocal images were collected with a Leica SP5 or an Olympus FLUOVIEW 1000 IX 81 microscope. Image processing was carried out with the ImageJ distribution Fiji (Schindelin et al., 2012), Leica LAS AF (2.3.5), Amira 4.0.01 (Mercury Computer Systems) and Adobe Photoshop. Measurement and counting of neurons and neuroblasts were carried out with Amira and Fiji, respectively. The diameter of Neurotactin (expressed at cell membranes)-stained embryonic neuroblasts and either Miranda or F-actin stained larval neuroblasts was estimated by focusing their center in *z*-axis and then calculating the average of the largest and smallest cell extension in *x*-/*y*-axis.

Immunoprecipitation

The vectors for transient expression of HA-tagged Mbt and 6xMyc-tagged Cdc42, Rac1, Rac2, Mtl, RhoA and RhoL in human embryonic kidney (HEK) 293 cells and the co-purification procedure have been described previously (Schneeberger and Raabe, 2003; Mentzel and Raabe, 2005).

Statistics

Data were analyzed with a two-tailed unpaired Student's *t*-test (SPSS 20V) except for Fig. 6K; Fig. 8C,E (Wilcoxon-Mann-Whitney U-test, RStudio 0.95.263) and Fig. 7E (Welch *t*-test, RStudio). In case of ties in the counting data, the package coin was used for calculation of exact *P* values for the Wilcoxon-Mann-Whitney U-test (RStudio).

RESULTS

Cell cycle-dependent localization of Mbt in central brain neuroblasts

To look for a function for Mbt in the developing CNS, we stained third instar larval brains with an antibody for Mbt (Schneeberger and Raabe, 2003) and analyzed the central brain area for Mbt localization. Co-stainings with the basal protein Miranda showed a pronounced enrichment of Mbt at the apical cortex of many central brain neuroblasts (Fig. 1A-A″). In the homozygous viable null allele mbt^{P1} (Schneeberger and Raabe, 2003) no Mbt expression was observed in neuroblasts (Fig. 1B-B″). As Mbt localized apically in only a fraction of neuroblasts, we checked for cell cycle-dependent distribution of Mbt. Larval brains were stained for γ-Tubulin and phospho-histone H3 (PH3) to distinguish cell cycle stages. In interphase neuroblasts, either weak cortical localization of Mbt (Fig. 1C, arrows) or a more pronounced basal staining was detected (Fig. 1D, arrow). Accumulation of apical Mbt protein started at prophase, reached a peak during metaphase and decreased during anaphase (Fig. 1E-H). Thus, the apical enrichment of Mbt is cell cycle dependent. This cell cycle dependent asymmetric accumulation of Mbt was also observed in embryonic brain neuroblasts and thus seems to be present throughout neural development (Fig. 1I,J).

Cortical localization of Mbt requires a functional RhoGTPase-binding site and is mediated by Cdc42

Binding of RhoGTPases to the p21-binding domain (PBD) of Mbt does not significantly enhance kinase activity but instead is essential for localization at adherens junctions during eye development (Schneeberger and Raabe, 2003). To test for the requirement of the

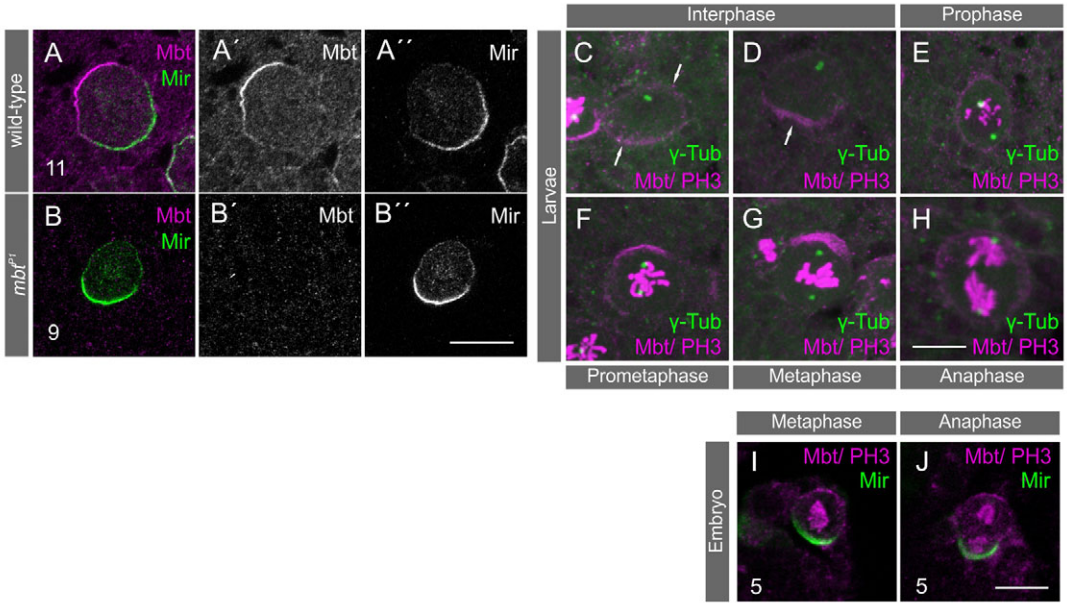

Fig. 1. Localization of Mbt in neuroblasts is cell cycle dependent. Projections of confocal sections of third instar brains stained for Mbt and Miranda (Mir) (A-B″) or Mbt, phospho-histone H3 (PH3) and γ-Tubulin (C-H). (I,J) Embryos were stained for Mbt, PH3 and Mir. Numbers in confocal images denote n as the number of scanned brains. The whole neuroblast population in each stack was analyzed and representative neuroblasts are shown. Apical is upwards. (**A-A″**) In wild-type brains, Mbt accumulates apically in neuroblasts. (**B-B″**) In mbt^{P1} brains, no Mbt can be detected. (**C-E**) Low levels of Mbt are detectable at the neuroblast cell cortex before metaphase (arrows). (**F-H**) During metaphase, Mbt shows a strong apical enrichment followed by a decrease of Mbt in anaphase. Eighteen hemispheres were analyzed for cell cycle-dependent Mbt localization. (**I**,**J**) The apical enrichment of Mbt is also seen in embryonic brain neuroblasts. Scale bars: 10 μm.

PBD or a functional kinase domain for the cortical and the pronounced apical Mbt localization in neuroblasts, we expressed wild-type or mutated *mbt* transgenes in mbt^{P1} animals with the neuroblast-specific *worniu-GAL4* driver line (Albertson and Doe, 2003). Expression of the wild type *mbt* transgene in mbt^{P1} animals resulted in the appearance of cortical Mbt and apical enriched Mbt protein in metaphase neuroblasts reflecting the localization of the endogenous Mbt protein (compare Fig. 2A-A″ and Fig. 1A-A″). The same result was observed with two different kinase-deficient Mbt proteins (Mbt^{K397M} and Mbt^{T525A}), demonstrating that kinase activity is not a prerequisite for apical Mbt localization (Fig. 2B-B″ and data not shown). By contrast, mutation of the PBD ($Mbt^{H19,22L}$) prevented apical enrichment of Mbt and resulted in elevated cytoplasmic levels of the protein (Fig. 2C-C″), thus confirming the requirement of the PBD for correct Mbt localization.

PAK proteins interact selectively with RhoGTPases in their GTP-bound active conformation, most prominently with Rac and/or Cdc42 subclass members. Six different RhoGTPases have been described in *Drosophila*: Cdc42, Rac1, Rac2, the related Mtl protein, RhoA and RhoL. We extended our previous binding studies of Mbt to RhoGTPases (Schneeberger and Raabe, 2003) and could show that Mbt can be selectively co-immunoprecipitated with Cdc42 upon heterologous expression in human HEK293 cells (Fig. 2D).

To verify these findings *in vivo*, the loss-of function mutation $Cdc42^{3}$ (Genova et al., 2000) was analyzed for its ability to interfere with cortical or apical localization of Mbt in metaphase neuroblasts. In homozygous $Cdc42^{3}$ second instar brains stained for Mbt, γ-Tubulin and PH3, no cortical or apical Mbt protein could be detected in neuroblasts (Fig. 2E-E″). Ubiquitous expression of the *Cdc42* transgene in a $Cdc42^{3}$ background restored cortical Mbt and the apical Mbt crescent, thus confirming the requirement of Cdc42 for Mbt localization (Fig. 2F-F″). These experiments demonstrated that the same molecular interaction is required to localize Mbt at adherens junctions in the developing eye (Schneeberger and Raabe, 2003) and at the cortex of central brain neuroblasts.

Mbt does not affect asymmetric cell division or the cytoskeleton in neuroblasts

The apical enrichment of Mbt in metaphase neuroblasts raises the issue of whether loss of *mbt* function interferes with asymmetric cell division of neuroblasts. Basically, there are two apical protein complexes regulating asymmetric division: the Par protein complex and a Pins-associated protein complex. On the basal side, there are two more protein complexes, the Miranda and the Numb-Pon complex (Doe, 2008; Knoblich, 2010). Failure in the establishment of cell polarity in the dividing neuroblast and in the correct orientation of the mitotic spindle, and the unequal distribution of cell fate determinants can impinge on the ability of neuroblasts to self-renew and to generate a further differentiated GMC during asymmetric cell division, which may result in deregulation of cell proliferation (Chia et al., 2008; Wu et al., 2008). When stained for aPKC, Numb, Miranda and Pins as representative members of each complex, no change of the localization patterns was observed in mbt^{P1} neuroblasts compared with wild-type neuroblasts (Fig. 3A-F). Moreover, orientation of the mitotic spindle along the polarity axis was undisturbed in the mutant (Fig. 3G,H). Cell size asymmetry upon division was maintained in embryonic and larval mbt^{P1} neuroblasts (Fig. 3I-L), and segregation of the cell fate determinant Miranda into the GMC was also undisturbed in both embryos and larvae (Fig. 3K,L).

The asymmetric localization of cell fate determinants depends on the actin cytoskeleton (Broadus and Doe, 1997; Knoblich et al., 1997). The correct localization of cell fate determinants in mbt^{P1} neuroblasts indicates that the actin cytoskeleton is intact. Yet PAK

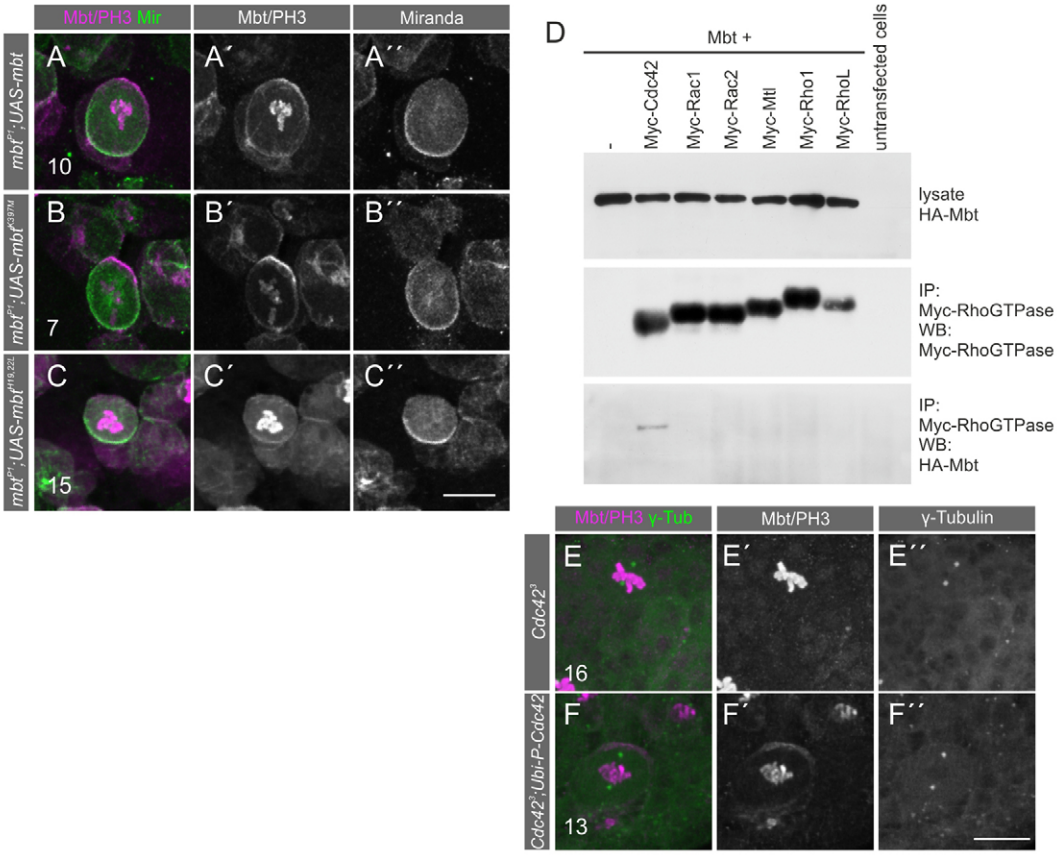

Fig. 2. Localization of Mbt requires a functional RhoGTPase binding domain and is mediated by Cdc42. Projections of confocal sections of third instar brains stained for Mbt, PH3 and Mir. The indicated *mbt* transgenes were expressed in neuroblasts with *worniu-GAL4* in an mbt^{P1}-null mutant background. (**A-C″**) Wild-type (A-A″) and kinase-deficient (B-B″) versions of Mbt are enriched at the apical cortex of metaphase neuroblasts like the endogenous Mbt protein (see Fig. 1). By contrast, the RhoGTPase-binding deficient $Mbt^{H19,22L}$ protein shows a pronounced cytoplasmic localization (C-C″). (**D**) HEK293 cells were transfected with *HA-mbt* alone or together with constructs for different Myc-tagged RhoGTPases. Lysates were subjected to co-immunoprecipitations with anti-Myc (IP) and analyzed by western blot (WB) using anti-Myc and anti-HA antibodies. Only Cdc42 precipitates Mbt (n=2). (**E-F″**) Second instar brains stained for Mbt, PH3 and γ-Tubulin. In *Cdc42*-deficient brains ($Cdc42^3$), no cortical accumulation of Mbt was detected in neuroblasts (E-E″). Expression of a *Cdc42* transgene under the ubiquitin promotor (*Ubi-P-Cdc42*) in a $Cdc42^3$ background restored Mbt at the apical cortex (F-F″). Scale bars: 10 μm. Numbers in confocal images denote n as the number of scanned brains. The whole neuroblast population in each stack was analyzed and representative neuroblasts are shown. Apical is upwards.

proteins are known to affect the actin and microtubule cytoskeleton via a number of effector pathways (reviewed by Arias-Romero and Chernoff, 2008; Eswaran et al., 2008; Wells and Jones, 2010). β-Catenin and its *Drosophila* homolog Armadillo, proteins that are also associated with the cytoskeleton, were recently identified as binding partners and phosphorylation substrates of PAK proteins (He and Baldwin, 2008; Menzel et al., 2008; Li et al., 2012). However, we did not observe significant changes in the localization patterns of F-actin (Fig. 4A-F′), α-Tubulin (Fig. 4G-N′) and Armadillo (Fig. 4O-T′) in mbt^{P1} neuroblasts during the cell cycle. Consistent with normal spindle orientation (Fig. 3G,H), astral microtubules are also apparently not affected (Fig. 4I′,J′,M′,N′, insets). Taken together, these findings argue against a major function of Mbt in the regulation of asymmetric cell division or the organization of microfilaments and microtubules in central brain neuroblasts.

Loss of *mbt* does not alter cell fate specification of embryonic MBNBs and Kenyon cells

Mbt is expressed in embryonic and postembryonic MBNBs (Fig. 1I,J; data not shown) and adult mbt^{P1} mutant brains exhibit a pronounced reduction of the overall mushroom body size owing to a reduced number of neurons (supplementary material Fig. S1A-B′) (Melzig et al., 1998). Both indicate a role in mushroom body (MB) development. In addition, MBNBs and their lineages are to date the only central brain neuroblast lineages characterized from their embryonic origin until the imago, making them an ideal model system (Kunz et al., 2012). In each brain hemisphere, four MBNBs continuously divide from embryonic until late pupal stages to generate all different subtypes of MB neurons (Kenyon cells) in a sequential manner (Ito and Hotta, 1992; Ito et al., 1997; Lee et al., 1999). The embryonic MBNBs are individually characterized by their enlarged size, their distinct position within the brain cortex and the specific expression of a set of transcription factors; thus, they are readily identifiable (Kunz et al., 2012). In stage 17 wild-type embryos, all MBNBs (labeled a-d, Fig. 5A-C″) and their progeny (that are γ-neurons in the embryo) expressed Eyeless (Ey). A subset of MBNBs (a-c) and part of their γ-neurons co-expressed Dachshund (Dac) (Fig. 5A-C″). The number and position of MBNBs, as well as the expression of Ey and Dac in MBNBs showed no difference in mbt^{P1} compared with the wild-

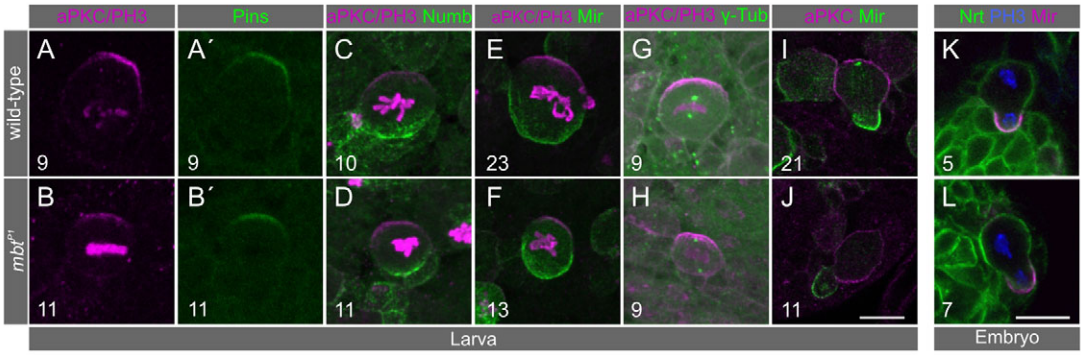

Fig. 3. Localization of protein complexes regulating asymmetric cell division is not altered in *mbt*^{P1} neuroblasts. Projections of confocal sections of wild-type and *mbt*^{P1} third instar brains co-stained for aPKC/PH3/Pins (A-B′), aPKC/PH3/Numb (C,D), aPKC/PH3/Mir (E,F), aPKC/PH3/γ-Tubulin (G,H) and aPKC/Mir (I,J). Embryos were stained for Nrt/PH3/Mir (K,L). (**A-F**) In metaphase, no difference in localization of cell fate determinants can be detected between wild type and *mbt* mutant. (**G**,**H**) Spindle orientation was undisturbed in *mbt*^{P1} neuroblasts. (**I**,**J**) Cell size asymmetry of neuroblast and GMC was unaffected in *mbt*^{P1} neuroblasts. (**K**,**L**) Cell size asymmetry of neuroblast and GMC, and segregation of Mir into the GMC were unaffected in embryonic *mbt*^{P1} neuroblasts. Scale bars: 10 μm. Numbers in confocal images denote n as the number of scanned brains. The whole neuroblast population in each stack was analyzed and representative neuroblasts are shown. Apical is upwards.

type embryos, and also Ey/Dac expression in the respective γ-neurons was largely normal, although their final number is reduced (Fig. 5D-F″). This indicates that formation of the correct MBNB number, as well as specification of MBNB and γ-neuron cell fate is principally not affected in the absence of Mbt. This is further confirmed by our observation that Tailless (Tll), which is specifically expressed in postembryonic MBNBs (and GMCs) (Kurusu et al., 2009), is unaltered in larval *mbt*^{P1} MBNBs (Fig. 6E).

Loss of Mbt decreases the mitotic activity of MBNBs

As MBNBs and Kenyon cells are correctly specified in *mbt*^{P1}, a defect in neuroblast or GMC proliferation and apoptosis, also of neurons, could account for the reduced neuron number in adult *mbt*^{P1} brains. In late stage 17 embryos, the total number of Ey^{+} daughter cells of MBNBs was significantly smaller in *mbt*^{P1} mutants compared with the wild type; this reduction concerned the Ey^{+}/Pros^{+} MBNB progeny, including GMCs (Ey^{+}/Pros^{+}/Elav^{-}) and newly born Kenyon cells (Ey^{+}/Pros^{+}/Elav^{+}), as well as the population of Ey^{+}/Dac^{+} Kenyon cells (Fig. 5; Fig. 6A,D and data not shown). Whereas the total number of four MBNBs per hemisphere was not altered in *mbt*^{P1} embryos, their overall mitotic activity, as verified by Ey^{+}/Deadpan^{+} (Dpn, a neuroblast marker)/PH3^{+} staining, was significantly decreased in the absence of Mbt (Fig. 6B,C). The reduction of mitotic activity was also seen at the single MBNB level as exemplified for MBNBc (Fig. 6C). Corresponding to the decreased mitotic activity of MBNBs, the total number of GMCs, and, accordingly, the number of mitotic GMCs was reduced in *mbt*^{P1} mushroom bodies, as is also shown for the MBNBc lineage (Fig. 6D).

In case of larval MBNBs, the mitotic activity is reduced by half at 36, 48 and 96 hours ALH, as revealed in Tll^{+}/Dpn^{+}/PH3^{+} stainings (Fig. 6E,F). In addition, Tll^{+} was strongly reduced in *mbt*^{P1} MBNB daughter cells (Fig. 6E,G), suggesting that MBNBs generate less GMCs in the absence of Mbt. Taken together, these data indicate that Mbt is required for normal levels of proliferation in embryonic and larval MBNBs, and likely in other brain NBs. So far we cannot rule out the possibility that Mbt in addition promotes cell division in the GMCs of MBNBs.

Furthermore, for an analysis of the proliferation capacity of single postembryonic MBNBs we took advantage of their characteristic proliferation pattern by which each MBNB sequentially generates distinct Kenyon cell subtypes. The γ-neurons are generated from embryogenesis until mid-third larval instar, then α′/β′- neurons are born until late third larval instar, followed by α/β-neurons (Ito et al., 1997; Lee et al., 1999). In the adult brain, axons from γ-neurons form the medially projecting γ-lobe, whereas α′/β′- neurons and α/β-neurons bifurcate to build up the dorsally projecting α/α′-lobes and the medially projecting β/β′-lobes. Single MBNBs and their progeny were labeled from the beginning of larval hatching by the MARCM technique (Lee et al., 1999) and adult brains were analyzed with respect to their lobe composition and Kenyon cell number. In single MBNB control clones, all three lobe systems were present (Fig. 6H). In most *mbt*^{P1} neuroblast clones, γ-, α/α′- and β/β′-lobes were present but were severely reduced in size in comparison with the wild type (Fig. 6I). In some cases, only a strongly reduced γ-lobe developed (Fig. 6J). In compliance with this observation, *mbt*^{P1} clones contained significantly fewer neurons than control clones (Fig. 6K). These data support our observation that MBNBs proliferate at a reduced rate throughout development. Labeling single γ-neurons or α/β-neurons revealed no obvious morphological differences between control and *mbt*^{P1} Kenyon cells (Fig. 6L-O). In order to exclude apoptosis in neurons as a further cause of the adult MB phenotype, we expressed anti-apoptotic p35 with ey^{OK107} in *mbt*^{P1} Kenyon cells. No rescue of the reduced neuron number in the adult MB was observed (supplementary material Fig. S1C-D′). Supporting this finding, removal of one copy of the proapoptotic factors *grim*, *hid*, *rpr* and *sickle* with the deletion *Df(3L)H99* also failed to rescue the *mbt* MB phenotype (supplementary material Fig. S1E-F′).

In summary, these results demonstrate that Mbt function is not required for differentiation or survival of the different Kenyon cell subtypes. Instead, Mbt function is cell-autonomously required in MBNBs to control proliferation rate throughout development.

Mbt regulates neuroblast size in the embryonic and postembryonic brain

Several recent studies demonstrate a positive correlation between neuroblast proliferation and cell size (Maurange et al., 2008; Chell

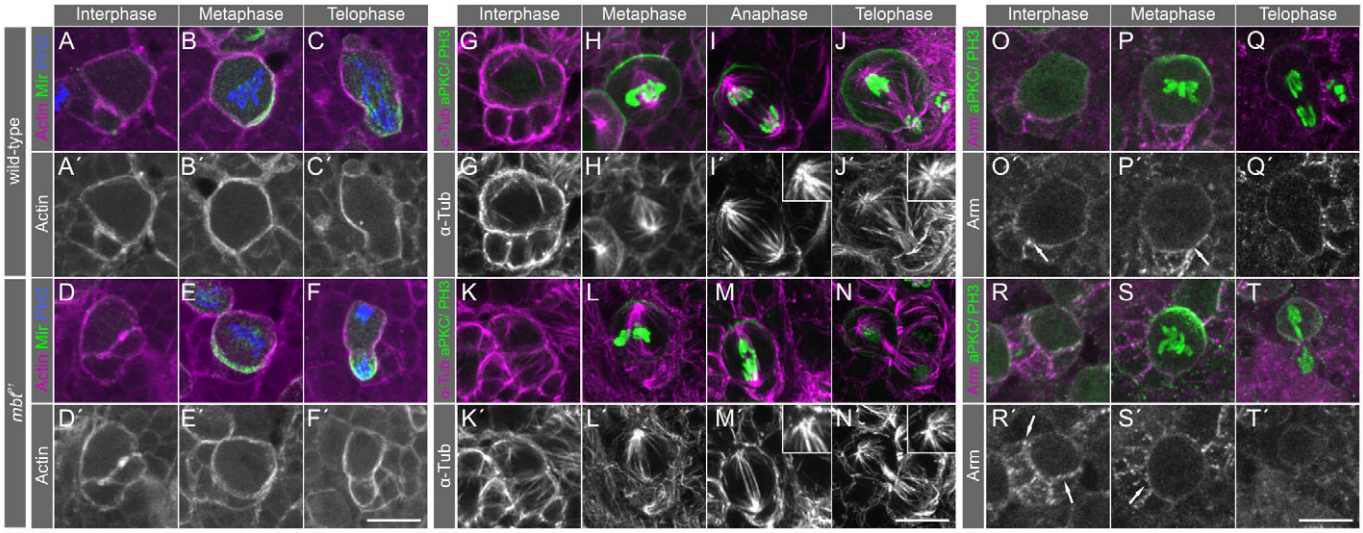

Fig. 4. Loss of Mbt does not disturb the cytoskeleton. Projections of confocal sections of third instar brains stained for either Actin/Mir/PH3, α-Tubulin (α-Tub)/aPKC/PH3 or Armadillo (Arm)/aPKC/PH3. Neuroblasts were analyzed for organization of the actin or α-Tubulin cytoskeleton or Armadillo localization. (**A-C′**) In wild-type neuroblasts, Actin is enriched at the cell cortex throughout the cell cycle. (**D-F′**) Loss of *mbt* does not affect cortical actin localization. (**G-N′**) At interphase α-Tub, as well as mitotic, spindles, appear undisturbed by loss of *mbt*. Insets show enlarged astral microtubules. (**O-T′**) Armadillo accumulates frequently at the neuroblast/GMC interface (arrows), but slight Armadillo staining is also detectable in the entire cortex, in both wild type and mbt^{P1}. At least 10 brains were analyzed for each staining and genotype. Scale bars: 10 μm. The whole neuroblast population in each stack was analyzed and representative neuroblasts are shown.

and Brand, 2010; Siegrist et al., 2010). In order to investigate whether the reduced proliferation in mbt^{P1} neuroblasts is also accompanied by a reduction in cell size, we first measured the diameter of each of the individually identifiable MBNBs (Fig. 7A,B) and of other brain neuroblasts at embryonic stage 17. The cell size of each MBNB as well as of the other neuroblasts was significantly reduced in mbt^{P1} brains (Fig. 7C,D). Next, we measured the diameter of MBNBs and other brain neuroblasts during larval development at 36, 48 and 96 hours ALH. As is summarized in Fig. 7D, at all investigated stages the diameter of neuroblasts (MBNBs and other neuroblasts) was significantly reduced in mbt^{P1} brains. Even though mbt^{P1} neuroblasts were always smaller than wild-type neuroblasts, they continuously gained size during larval development. Interestingly, MBNBs, which during larval development were always larger than other neuroblasts, became more severely reduced in cell size than other neuroblasts in mbt^{P1} brains during larval development. We also tested the diameter of larval GMCs generated by MBNBs at 96 hours ALH (when mbt^{P1} MBNBs show the strongest reduction in proliferation), which appeared slightly reduced compared with wild type.

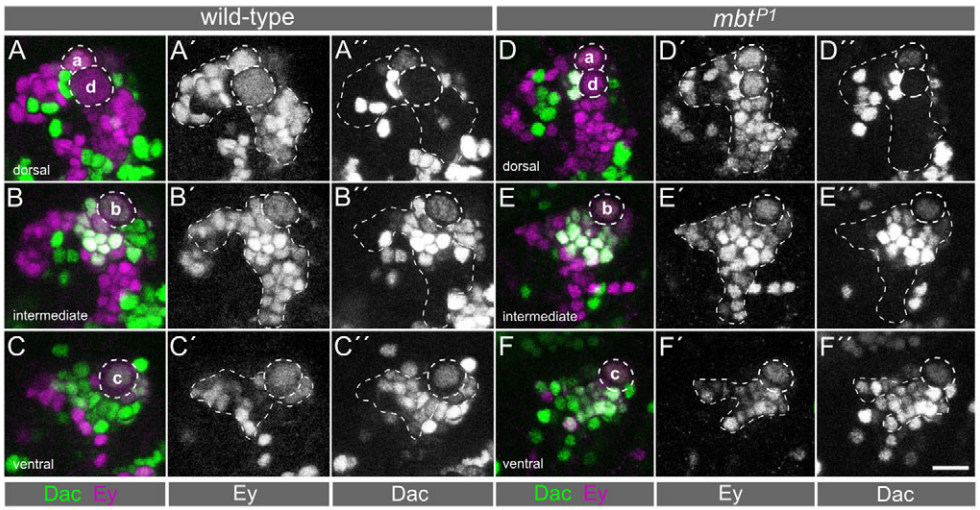

Fig. 5. Loss of Mbt does not alter cell fate specification of embryonic MBNBs and Kenyon cells. (**A-F″**) Composite confocal images of stainings against the transcription factors Eyeless (Ey) and Dachshund (Dac) showing the dorsal, intermediate and ventral parts of the mushroom body cortex in wild-type (A-C″) and mbt^{P1} brains (D-F″) at embryonic stage 17. The four embryonic MBNBs (indicated with a, b, c, d) and their daughter cells (γ-neurons, outlined with dashed lines in A′-F′) properly express Ey (for quantification of Ey^+ in Kenyon cells and MBNBs, see Fig. 6A,C). MBNBa, MBNBb and MBNBc, and subsets of corresponding γ-neurons co-express Dac. In the absence of Mbt, expression of Ey and Dac is unaltered in the four MBNBs, but the number of Dac^+/Ey^+ γ-neurons is slightly reduced [27.2±2.6 in mbt^{P1} (n=18 hemispheres); 30.6±3.2 in wild type (n=15 hemispheres); $^{**}P<0.01$]. Scale bar: 10 μm.

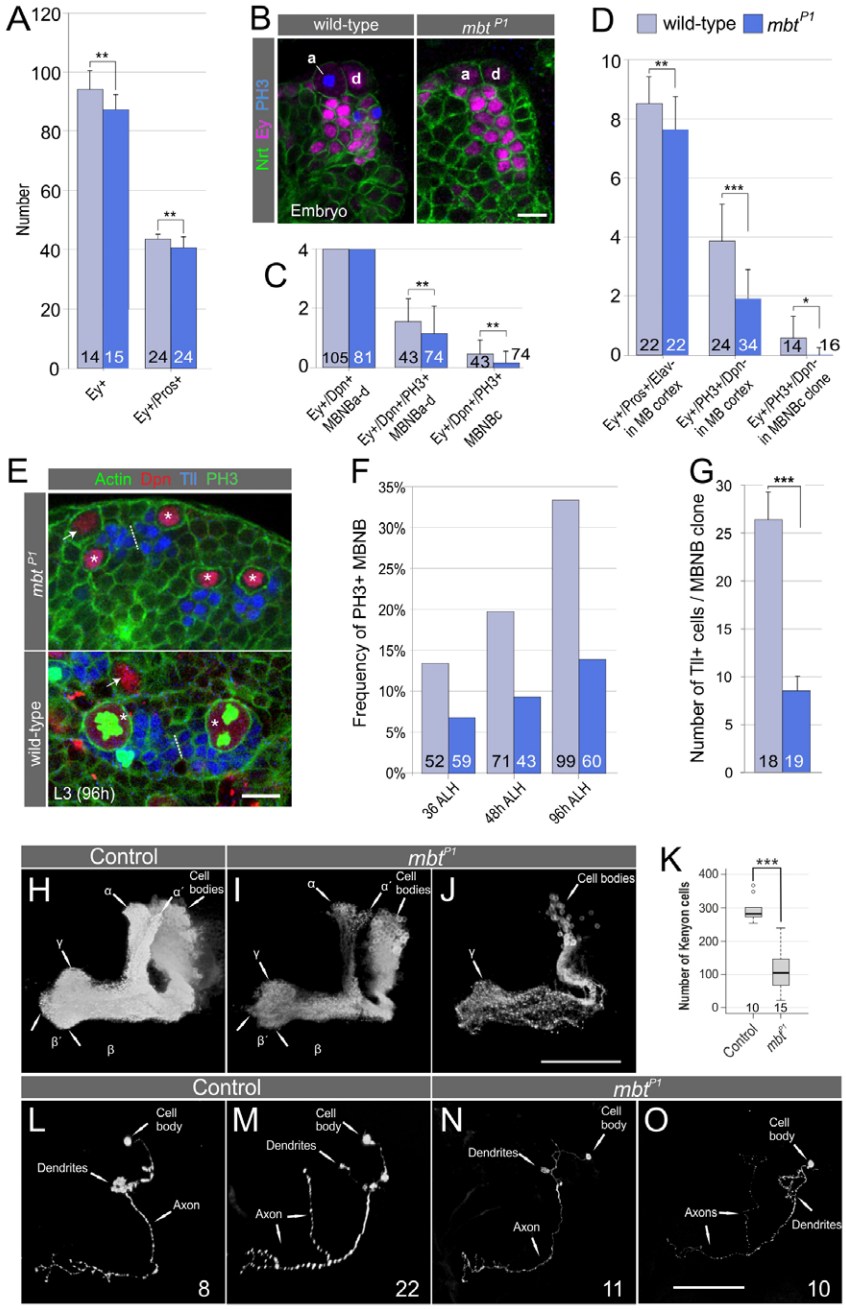

Fig. 6. Loss of Mbt leads to a decrease in the mitotic activity of MBNBs. Numbers in columns denote the number of hemispheres analyzed (A,C,D), the numbers of MBNBs (F) and the numbers of MBNB clones (G). (**A**) Number of Ey$^+$ daughter cells of MBNBs, as well as of Ey$^+$/Pros$^+$ MBNB daughter cells (that include GMCs and newly born Kenyon cells) is significantly smaller in *mbt* mutant embryos at late stage 17 (left columns: Ey$^+$ in wild type. (**B**) Composite confocal images of a Nrt$^+$/Ey$^+$/PH3$^+$stained embryonic MB cortex (stage 17) disclosing mitotic MBNBs and GMCs. MBNBa (a) and MBNBd (d) are indicated in the wild-type (left) and *mbt* mutant (right) MB cortex. Scale bar: 10 µm. (**C**) The total number of the four embryonic MBNBs (Ey$^+$/Dpn$^+$) is unaltered in *mbt* mutant embryos (left). The mitotic activity of all four MBNBs (Ey$^+$/Dpn$^+$/PH3$^+$) is significantly decreased, as is scored in detail for MBNBc. (**D**) The total number of GMCs (Ey$^+$/Pros$^+$/Elav$^-$) in the MB cortex and, correspondingly, the number of mitotic GMCs (Ey$^+$/PH3$^+$/Dpn$^-$) is reduced in *mbt^{P1}* brains, as additionally shown for the lineage of MBNBc. (**E**) Composite confocal images of the larval MB cortex stained against Actin$^+$/Dpn$^+$/Tll$^+$/PH3$^+$. Cell size (outlined by Actin$^+$) of all four MBNBs (Tll$^+$/Dpn$^+$) in *mbt^{P1}* (asterisks) is smaller compared with two mitotic MBNBs (Tll$^+$/Dpn$^+$/PH3$^+$) in wild type; number of Tll$^+$ MBNB daughter cells is reduced in *mbt^{P1}*. Arrows indicate other brain neuroblasts. Scale bar: 10 µm. (**F**) Frequency of mitotic (PH3$^+$) MBNBs is strongly reduced at 36, 48 and 96 hours ALH in *mbt^{P1}* mutant brains. (**G**) Accordingly, the average number of Tll$^+$ MBNB daughter cells is strongly reduced in *mbt^{P1}* at 96 hours ALH (compare with E). (H-K) Single control or homozygous *mbt^{P1}* MBNB clones were induced at first larval instar. Control and *mbt^{P1}* homozygous cells were marked by concomitant expression of the *UAS-mCD8::GFP* reporter with the *ey^{OK107}* and were visualized in the adult brain by staining for GFP. (**H**) In a control neuroblast clone, the lobe subdivision indicates the generation of γ-, α′/β′- and α/β-neurons. Kenyon cell bodies are located in the dorsal cortex. (**I**,**J**) In *mbt^{P1}* MBNB clones, which correspond to the reduced number of Kenyon cells, either a largely reduced lobe system (I) or only γ-lobes (J) develop. (**K**) Quantification of Kenyon cells generated by a single MBNB; numbers indicate MARCM clones analyzed. (**L-O**) *mbt^{P1}* does not influence the morphology of different Kenyon cell subtypes. Neither γ-neurons generated during early larval stages (L,N) nor α/β- neurons, which are born during pupal development (M,O), show differences from the wild-type projection pattern. Numbers indicate MARCM clones analyzed. Scale bars: 50 µm. Error bars indicate s.d., *P<0.05; **P<0.01; ***P<0.0001.

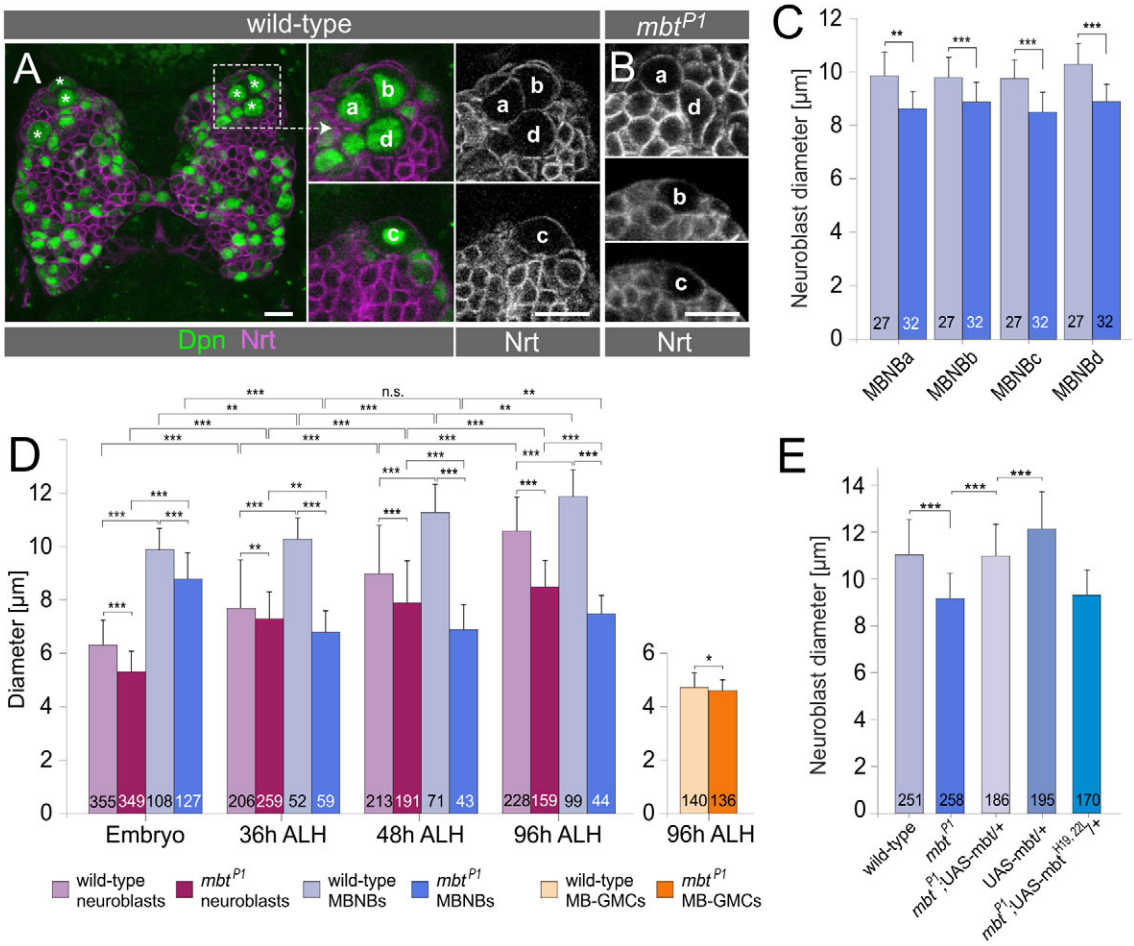

Fig. 7. Mbt regulates neuroblast size. (**A**) Composite confocal images of a wild-type brain at embryonic stage 17 stained against Dpn$^+$ /Nrt$^+$. The MBNBs indicated with asterisks are individually assigned with a, b, c, d in the higher magnifications (middle panels). (**B**) Composite confocal images of corresponding cortical areas in the *mbt* mutant brain. Scale bars: 10 µm. (**C**) Diameter of each of the four MBNBs (a-d) is significantly reduced at embryonic stage 17. (**D**) Left: the diameter of neuroblasts (MBNBs and other neuroblasts) is significantly reduced in embryonic (stage 17) and larval (36, 48 and 96 hours ALH) *mbt*^{P1} brains. Note that the size of MBNBs is diminished even more than that of other neuroblasts in *mbt*^{P1} larval brains. Right: The diameter of *mbt*^{P1} GMCs produced by MBNBs (MB-GMCs) is slightly reduced at 96 hours ALH. Only those three to five Tll$^+$ GMCs lying closest to the Tll$^+$/Dpn$^+$ MBNB of origin were scored. Numbers in columns denote numbers of neuroblasts or GMCs, respectively. (**E**) At 96 hours ALH, wild-type neuroblast size was restored by *worniu-GAL4* driven expression of a wild-type *mbt*-transgene in an *mbt*^{P1} background. Expression of the *mbt*-transgene in wild-type background resulted in increased neuroblast size compared with the wild type. Expression of *mbt*^{H19,22L} in *mbt*^{P1} animals resulted in a marginal increase of neuroblast size compared with *mbt*^{P1} (*mbt*^{P1}: 9.15±1.05, *mbt*^{P1}*; mbt*^{H19,22L}/+: 9.35±1.04, *P*=0.053). Error bars indicate s.d.; n.s., not significant, ***P*<0.01;****P*<0.0001.

To attribute the cell size defect in *mbt*^{P1} neuroblasts specifically to the loss of Mbt function, rescue and overexpression experiments were performed. Neuroblast-specific expression of a wild-type *mbt*-transgene with *worniu-GAL4* in a *mbt*^{P1} background restored the wild-type size of neuroblasts in 96-hour-old larvae (Fig. 7E) and rescued the adult MB phenotype (supplementary material Fig. S1A,A′,G,G′). Overexpression of this *mbt* transgene in the wild-type background resulted in neuroblasts slightly larger than in the wild type (Fig. 7E) without affecting the adult MB structure (supplementary material Fig. S1H,H′). This supports a function of Mbt in cell growth control. Expression of the localization-deficient but otherwise fully functional Mbt^{H19,22L} protein resulted in a slight increase of cell size (Fig. 7E, *P*=0.053) and correspondingly to a partial rescue of the adult MB (supplementary material Fig. S1I,I′) emphasizing the importance of correct cortical localization for full Mbt function.

Altogether, these data indicate that Mbt is needed to control proper cell size of embryonic and larval brain neuroblasts, and GMCs. Moreover, they suggest that the impact of Mbt on cell size is much stronger in MBNBs than in other brain NBs.

Mbt regulates neuroblast number throughout postembryonic brain development

A reduction in cell size implicates a decline of proliferation and may result in the subsequent termination of neuroblast proliferation by either apoptosis or terminal differentiation (Maurange et al., 2008; Siegrist et al., 2010). In order to investigate whether in *mbt*^{P1} brains reduced cell size and proliferation are followed by a subsequent, premature loss of neuroblasts, we determined the MBNB and the total neuroblast number per hemisphere at different developmental stages. In wild type, the four MBNBs in each hemisphere are present from the embryo until pupal stages before they disappear

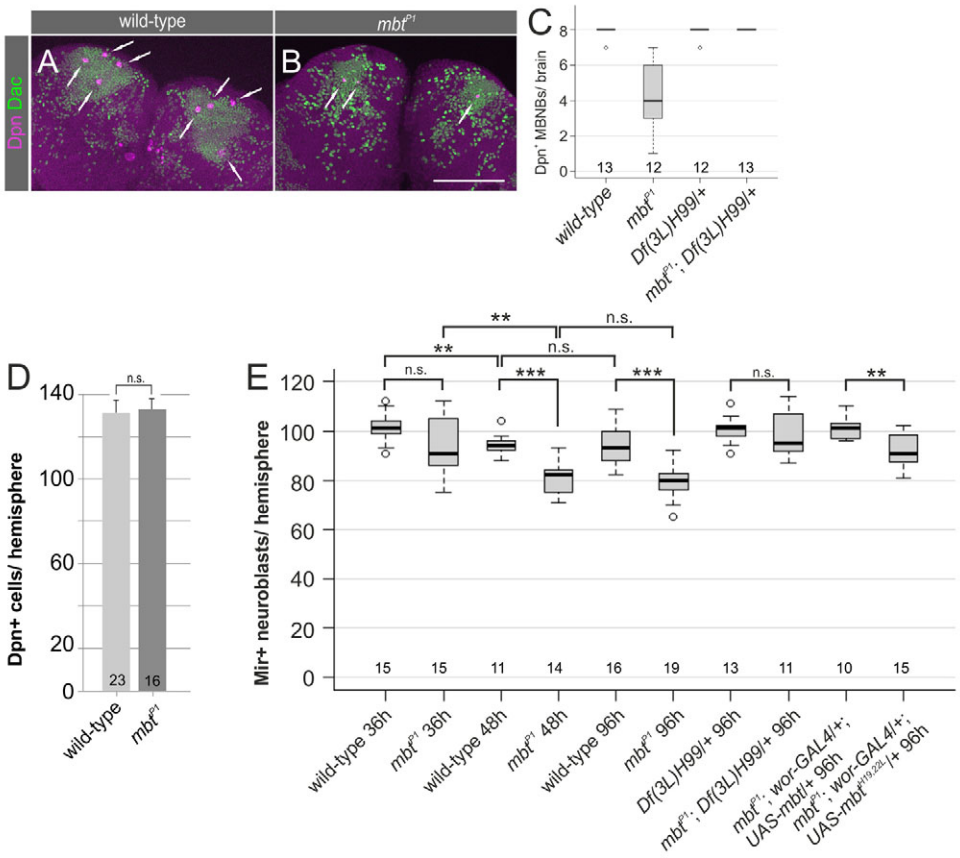

Fig. 8. Loss of Mbt affects neuroblast number in the postembryonic brain. (**A**,**B**) Projections of confocal sections of pupal brains 48 hours APF stained for Dpn and Dac. Scale bar: 100 µm. (**C**) The number of MBNBs is reduced in mbt^{P1} pupal brains. *Df(3L)H99* restores wild-type MBNB numbers. *Df(3L)H99/+* is the corresponding control. (**D**) The total number of Dpn^+ cells in stage 17 brains is unaltered in mbt^{P1} embryos (133.3±5.3) when compared with the wild type (131.7±6.4; P=0.43). The number of Dpn^+ cells is higher than the total number of brain neuroblasts scored at embryonic stage 11 (Urbach et al., 2003), because during later development Dpn is additionally expressed in transit-amplifying neural progenitors (e.g. Bello et al., 2008; Hwang and Rulifson, 2011) and transiently in newly formed GMCs (K.F.K. and R.U., unpublished). (**E**) In 36-hour-old larvae, the number of Mir^+ neuroblasts does not differ between control and mbt^{P1} brains. In 48- and 96-hour-old larvae, mbt^{P1} brains contain fewer neuroblasts than the wild type. *Df(3L)H99* suppresses the loss of neuroblast number in mbt^{P1} and shows no significant difference to the corresponding control. Although the *mbt* and the $mbt^{H19,22L}$ transgenes increase neuroblast numbers, they significantly differ from each other. Error bars indicate s.d.; n.s., not significant, $^{**}P<0.01$, $^{***}P<0.0001$.

about 96 hours after puparium formation (APF) (Ito and Hotta, 1992; Siegrist et al., 2010). In mbt^{P1} brains, the number of MBNBs is unchanged from the embryo to late larval stages (Fig. 6C,E and data not shown). However, at 48 hours APF, when wild-type brains still contain eight MBNBs (Fig. 8A,C), the number of MBNBs is prematurely reduced (Fig. 8B,C). Blocking apoptosis by introducing one copy of the *Df(3L)H99* into an mbt^{P1} mutant background restored the wild-type MBNB number (Fig. 8C). Even though blocking apoptosis suppresses the premature loss of MBNBs, this is not sufficient to restore the wild-type MB structure (supplementary material Fig. S1E-F′).

Looking at the overall neuroblast population, the total number of Dpn-positive cells did not vary between wild-type and mbt^{P1} brains in stage 17 embryos (Fig. 8D). In addition, at 36 hours ALH, no significant difference in the number of neuroblasts was observed (Fig. 8E). In wild-type, as well as in mbt^{P1}, brains, neuroblast numbers decreased between 36 and 48 hours ALH. However, at 48 hours ALH, the neuroblast number was already significantly lower in the *mbt* mutant than in the wild type, indicating a premature loss of neuroblasts (Fig. 8E). About the same difference in neuroblast number was observed at 96 hours ALH (Fig. 8E). Suppression of apoptosis by *Df(3L)H99* restored the number of neuroblasts in 96-hour larvae to wild-type levels (Fig. 8E). Likewise, *worniu-GAL4* driven expression of a wild-type *mbt*-transgene completely reverted the mbt^{P1} neuroblast number defect (Fig. 8E). Interestingly, the localization-deficient, but otherwise functional, $Mbt^{H19,22L}$ protein also increased neuroblast number. However, the number remained significantly smaller compared with the wild-type *mbt* transgene (Fig. 8E). Despite the significant increase in neuroblast number, only a partial rescue of the adult MB structure was observed (supplementary material Fig. S1I,I′).

Taken together, these experiments support the conclusion that reduced neuroblast size and proliferation are followed by premature loss of neuroblasts due to apoptosis. In the case of MBNBs, apoptosis is not the primary cause of the adult *mbt* brain phenotype. Instead, impaired proliferation activity of MBNBs seems to be the relevant factor.

DISCUSSION

Mbt mutant brains are characterized by decreased size of central brain tissues, of which the mushroom bodies show the most pronounced reduction (Melzig et al., 1998). In this study, we

demonstrate that *mbt* mutant MBNBs and their progeny express their characteristic combination of transcription factors and, thus, show correct cell fate specification (Kunz et al., 2012). They can sequentially generate all different Kenyon cell subtypes, which differentiate properly and survive until adulthood. This argues against a major function of Mbt in these developmental processes. Moreover, as the overall morphology of Kenyon cells is not disturbed in *mbt* mutants, Mbt seems also not to be required for the establishment of their axonal projections, which is in contrast to the function reported for PAK1 (Ng and Luo, 2004). The undisturbed Kenyon cell morphology in mbt^{P1} mutants also allows for the conclusion that Mbt is not involved in their reorganization during metamorphosis. Instead, we provide evidence that the mbt^{P1} mushroom body phenotype results from impaired neuroblast proliferation. Embryonic, as well as postembryonic, mbt^{P1} MBNBs showed reduced mitotic activity and accordingly, produced less progeny. Finally, MBNBs are lost prematurely from mbt^{P1} brains owing to apoptosis. However, apoptosis is not the primary cause of the adult mushroom body phenotype.

Our observation that neuroblast size is significantly decreased in *mbt* mutants could provide an explanation for impaired neuroblast proliferation. Neuroblasts first enlarge before they re-enter the cell cycle after quiescence and inhibition of neuroblast growth prevents proliferation (Truman and Bate, 1988; Chell and Brand, 2010). In a mammalian cell culture system it was shown that the probability for cell division increases with cell size (Tzur et al., 2009). Mutations in the gene *Gβ13F* were also shown to affect cell size and proliferation (Fuse et al., 2003; Yu et al., 2003). These findings suggest a critical, minimal cell size required for cell division. Furthermore, embryonic, as well as larval, neuroblasts exhibit a progressive decrease in cell size before they first reduce and subsequently terminate their proliferative activity in late embryogenesis and larval development, respectively (Hartenstein et al., 1987; Truman and Bate, 1988; Maurange et al., 2008; Siegrist et al., 2010). Thus, a reduction in cell growth affects proliferation. Supporting this notion, embryonic and larval *mbt* MBNBs (as well as other brain neuroblasts) are always smaller than wild-type neuroblasts although they slightly increase size during larval development (Fig. 7D). This raises the question why does *mbt* mutation severely affect mushroom body development (Melzig et al., 1998) despite its expression also in other central brain neuroblasts? Indeed, MBNBs show a much more pronounced cell size defect than the remaining NBs (Fig. 7D).

What could be the downstream targets for Mbt function in neuroblasts? Although PAK proteins are involved in reorganization of the cytoskeleton, we did not detect obvious defects in the distribution of F-actin and microtubules in *mbt* neuroblasts. In addition, asymmetric cell division is apparently not affected. Our finding that Cdc42 is the major component regulating Mbt enrichment at the apical cortex fits with the previous analysis of Cdc42 in larval brains where it accumulates at the apical cortex of dividing neuroblasts (Atwood et al., 2007). Based on loss-of-function and mis-expression experiments, it was concluded that localized Cdc42 activity is required for normal apical Par6 and aPKC localization. Likewise, Mbt binds Cdc42 only in the GTP-bound, active conformation (Schneeberger and Raabe, 2003) and Cdc42 is required for Mbt accumulation at the apical cortex of neuroblasts. The fact that we did not observe localization defects of aPKC and downstream targets such as Numb in *mbt* mutants argues against a major function of Mbt in Cdc42-regulated cell polarity.

Insulin signaling has long been known to act in the growth regulation of cells, tissues and whole organisms (Grewal, 2009; Teleman, 2009). Recent studies showed that insulin signaling regulates neuroblast reactivation after quiescence and the timely termination of neuroblast proliferation (Chell and Brand, 2010; Siegrist et al., 2010). During reactivation, insulin signaling initiated an increase in neuroblast size that was required for neuroblasts to enter mitosis (Chell and Brand, 2010). Activation of insulin signaling, in combination with inhibition of apoptosis, resulted in neuroblast survival, increased neuroblast size and prolonged proliferation (Siegrist et al., 2010). In another study, vertebrate PAK1 was shown to link insulin and Wnt signaling (Sun et al., 2009). Knockdown of PAK1 leads to decreased β-catenin phosphorylation at serine 675 upon insulin stimulation and thereby inhibits β-catenin dependent transcription. As a result, cell proliferation is blocked. Mbt is known to phosphorylate Armadillo, the *Drosophila* β-catenin ortholog, *in vitro* at the corresponding serine residue (Menzel et al., 2008). We therefore tested for genetic interaction between mbt^{P1} and mutations in various components of the insulin signaling pathway but found no enhancement or suppression of the *mbt* brain phenotype. In the case of *armadillo* mutations, we only observed a modification of the *mbt* rough eye phenotype, which fits with the requirement of Mbt in organization of adherens junctions during eye development (J.M. and T.R., unpublished observations). In addition, no obvious changes in the localization pattern of Armadillo in neuroblasts were detected (Fig. 4). Although our experiments do not formally exclude Mbt as a regulator of insulin and Wnt signaling, they at least strongly argue against a major impact of Mbt. Instead, our results suggest a new function of Mbt in neuroblasts, different from the one of PAK4 in mouse neural progenitor cells. In a recent study, knockout of murine PAK4, the vertebrate Mbt ortholog, caused a decrease in the number of neural progenitor cells owing to loss of β-catenin and neuroepithelial junctions (Tian et al., 2011).

One attractive hypothesis integrating all our findings would be that activated Cdc42 binds and anchors Mbt at the cortex of neuroblasts. Apical enrichment of Cdc42 ensures that the majority of Mbt protein remains within the daughter neuroblast, thus allowing for proper cell growth and repeated cell divisions. Analysis of the temporal regulation of Mbt activity during the cell cycle and identification of downstream targets will help to verify this model. In conclusion, we have identified the PAK protein Mbt as a new regulator of cell size, which influences the proliferation potential and survival of central brain neuroblasts.

Acknowledgements

We thank Patrick Callaerts, William Chia, Rick Fehon, Jürgen Knoblich, Liqun Luo, Fumio Matsuzaki, Hanh T. Nguyen, John Reinitz, James Skeath, Hugo Stocker, Uwe Walldorf and Daisuke Yamamoto for fly stocks, antibodies and many helpful suggestions. We also thank the Bloomington Drosophila Stock Center, Developmental Studies Hybridoma Bank and FlyBase for providing reagents and resources. Finally, we thank Heike Wecklein and Dagmar Volland for excellent technical assistance and Stefanie Pütz for discussions.

Funding

This work was supported by grants from the Deutsche Forschungsgemeinschaft [SFB487/C5 and Ra561/5-3 to T.R., UR163/2-1 and UR163/3-1 to R.U.] and by a research stipend (to K.F.K.) from the FTN of the University Mainz.

Competing interests statement

The authors declare no competing financial interests.

Supplementary material

Supplementary material available online at
http://dev.biologists.org/lookup/suppl/doi:10.1242/dev.088435/-/DC1

References

Albertson, R. and Doe, C. Q. (2003). Dlg, Scrib and Lgl regulate neuroblast cell size and mitotic spindle asymmetry. *Nat. Cell Biol.* **5**, 166-170.

Albin, S. D. and Davis, G. W. (2004). Coordinating structural and functional synapse development: postsynaptic p21-activated kinase independently specifies glutamate receptor abundance and postsynaptic morphology. *J. Neurosci.* **24**, 6871-6879.

Arias-Romero, L. E. and Chernoff, J. (2008). A tale of two Paks. *Biol. Cell* **100**, 97-108.

Atwood, S. X., Chabu, C., Penkert, R. R., Doe, C. Q. and Prehoda, K. E. (2007). Cdc42 acts downstream of Bazooka to regulate neuroblast polarity through Par-6 aPKC. *J. Cell Sci.* **120**, 3200-3206.

Bello, B. C., Hirth, F. and Gould, A. P. (2003). A pulse of the Drosophila Hox protein Abdominal-A schedules the end of neural proliferation via neuroblast apoptosis. *Neuron* **37**, 209-219.

Bello, B. C., Izergina, N., Caussinus, E. and Reichert, H. (2008). Amplification of neural stem cell proliferation by intermediate progenitor cells in Drosophila brain development. *Neural Dev.* **3**, 5.

Britton, J. S. and Edgar, B. A. (1998). Environmental control of the cell cycle in Drosophila: nutrition activates mitotic and endoreplicative cells by distinct mechanisms. *Development* **125**, 2149-2158.

Broadus, J. and Doe, C. Q. (1997). Extrinsic cues, intrinsic cues and microfilaments regulate asymmetric protein localization in Drosophila neuroblasts. *Curr. Biol.* **7**, 827-835.

Chan, P. M. and Manser, E. (2012). PAKs in human disease. *Prog. Mol. Biol. Transl. Sci.* **106**, 171-187.

Chell, J. M. and Brand, A. H. (2010). Nutrition-responsive glia control exit of neural stem cells from quiescence. *Cell* **143**, 1161-1173.

Chia, W., Somers, W. G. and Wang, H. (2008). Drosophila neuroblast asymmetric divisions: cell cycle regulators, asymmetric protein localization, and tumorigenesis. *J. Cell Biol.* **180**, 267-272.

Doe, C. Q. (2008). Neural stem cells: balancing self-renewal with differentiation. *Development* **135**, 1575-1587.

Eswaran, J., Soundararajan, M., Kumar, R. and Knapp, S. (2008). UnPAKing the class differences among p21-activated kinases. *Trends Biochem. Sci.* **33**, 394-403.

Fuse, N., Hisata, K., Katzen, A. L. and Matsuzaki, F. (2003). Heterotrimeric G proteins regulate daughter cell size asymmetry in Drosophila neuroblast divisions. *Curr. Biol.* **13**, 947-954.

Genova, J. L., Jong, S., Camp, J. T. and Fehon, R. G. (2000). Functional analysis of Cdc42 in actin filament assembly, epithelial morphogenesis, and cell signaling during Drosophila development. *Dev. Biol.* **221**, 181-194.

Grewal, S. S. (2009). Insulin/TOR signaling in growth and homeostasis: a view from the fly world. *Int. J. Biochem. Cell Biol.* **41**, 1006-1010.

Hartenstein, V., Rudloff, E. and Campos-Ortega, J. A. (1987). The pattern of proliferation of the neuroblasts in the wild-type embryo of Drosophila-melanogaster. *Rouxs Arch. Dev. Biol.* **196**, 473-485.

He, H. and Baldwin, G. S. (2008). Rho GTPases and p21-activated kinase in the regulation of proliferation and apoptosis by gastrins. *Int. J. Biochem. Cell Biol.* **40**, 2018-2022.

Hwang, H. J. and Rulifson, E. (2011). Serial specification of diverse neuroblast identities from a neurogenic placode by Notch and Egfr signaling. *Development* **138**, 2883-2893.

Ito, K. and Hotta, Y. (1992). Proliferation pattern of postembryonic neuroblasts in the brain of Drosophila melanogaster. *Dev. Biol.* **149**, 134-148.

Ito, K., Awano, W., Suzuki, K., Hiromi, Y. and Yamamoto, D. (1997). The Drosophila mushroom body is a quadruple structure of clonal units each of which contains a virtually identical set of neurones and glial cells. *Development* **124**, 761-771.

Knoblich, J. A. (2010). Asymmetric cell division: recent developments and their implications for tumour biology. *Nat. Rev. Mol. Cell Biol.* **11**, 849-860.

Knoblich, J. A., Jan, L. Y. and Jan, Y. N. (1997). The N terminus of the Drosophila Numb protein directs membrane association and actin-dependent asymmetric localization. *Proc. Natl. Acad. Sci. USA* **94**, 13005-13010.

Kreis, P. and Barnier, J. V. (2009). PAK signalling in neuronal physiology. *Cell. Signal.* **21**, 384-393.

Kunz, T., Kraft, K. F., Technau, G. M. and Urbach, R. (2012). Origin of Drosophila mushroom body neuroblasts and generation of divergent embryonic lineages. *Development* **139**, 2510-2522.

Kurusu, M., Maruyama, Y., Adachi, Y., Okabe, M., Suzuki, E. and Furukubo-Tokunaga, K. (2009). A conserved nuclear receptor, Tailless, is required for efficient proliferation and prolonged maintenance of mushroom body progenitors in the Drosophila brain. *Dev. Biol.* **326**, 224-236.

Lee, T., Lee, A. and Luo, L. (1999). Development of the Drosophila mushroom bodies: sequential generation of three distinct types of neurons from a neuroblast. *Development* **126**, 4065-4076.

Li, Y., Shao, Y., Tong, Y., Shen, T., Zhang, J., Li, Y., Gu, H. and Li, F. (2012). Nucleo-cytoplasmic shuttling of PAK4 modulates β-catenin intracellular translocation and signaling. *Biochim. Biophys. Acta* **1823**, 465-475.

Maurange, C., Cheng, L. and Gould, A. P. (2008). Temporal transcription factors and their targets schedule the end of neural proliferation in Drosophila. *Cell* **133**, 891-902.

Melzig, J., Rein, K. H., Schäfer, U., Pfister, H., Jäckle, H., Heisenberg, M. and Raabe, T. (1998). A protein related to p21-activated kinase (PAK) that is involved in neurogenesis in the Drosophila adult central nervous system. *Curr. Biol.* **8**, 1223-1226.

Mentzel, B. and Raabe, T. (2005). Phylogenetic and structural analysis of the Drosophila melanogaster p21-activated kinase DmPAK3. *Gene* **349**, 25-33.

Menzel, N., Schneeberger, D. and Raabe, T. (2007). The Drosophila p21 activated kinase Mbt regulates the actin cytoskeleton and adherens junctions to control photoreceptor cell morphogenesis. *Mech. Dev.* **124**, 78-90.

Menzel, N., Melzer, J., Waschke, J., Lenz, C., Wecklein, H., Lochnit, G., Drenckhahn, D. and Raabe, T. (2008). The Drosophila p21-activated kinase Mbt modulates DE-cadherin-mediated cell adhesion by phosphorylation of Armadillo. *Biochem. J.* **416**, 231-241.

Ng, J. and Luo, L. (2004). Rho GTPases regulate axon growth through convergent and divergent signaling pathways. *Neuron* **44**, 779-793.

Ozdowski, E. F., Gayle, S., Bao, H., Zhang, B. and Sherwood, N. T. (2011). Loss of Drosophila melanogaster p21-activated kinase 3 suppresses defects in synapse structure and function caused by spastin mutations. *Genetics* **189**, 123-135.

Parnas, D., Haghighi, A. P., Fetter, R. D., Kim, S. W. and Goodman, C. S. (2001). Regulation of postsynaptic structure and protein localization by the Rho-type guanine nucleotide exchange factor dPix. *Neuron* **32**, 415-424.

Schindelin, J., Arganda-Carreras, I., Frise, E., Kaynig, V., Longair, M., Pietzsch, T., Preibisch, S., Rueden, C., Saalfeld, S., Schmid, B. et al. (2012). Fiji: an open-source platform for biological-image analysis. *Nat. Methods* **9**, 676-682.

Schneeberger, D. and Raabe, T. (2003). Mbt, a Drosophila PAK protein, combines with Cdc42 to regulate photoreceptor cell morphogenesis. *Development* **130**, 427-437.

Siegrist, S. E., Haque, N. S., Chen, C. H., Hay, B. A. and Hariharan, I. K. (2010). Inactivation of both Foxo and reaper promotes long-term adult neurogenesis in Drosophila. *Curr. Biol.* **20**, 643-648.

Skeath, J. B. and Thor, S. (2003). Genetic control of Drosophila nerve cord development. *Curr. Opin. Neurobiol.* **13**, 8-15.

Sousa-Nunes, R., Yee, L. L. and Gould, A. P. (2011). Fat cells reactivate quiescent neuroblasts via TOR and glial insulin relays in Drosophila. *Nature* **471**, 508-512.

Sun, J., Khalid, S., Rozakis-Adcock, M., Fantus, I. G. and Jin, T. (2009). P-21-activated protein kinase-1 functions as a linker between insulin and Wnt signaling pathways in the intestine. *Oncogene* **28**, 3132-3144.

Teleman, A., A. (2009). Molecular mechanisms of metabolic regulation by insulin in Drosophila. *Biochem. J.* **425**, 13-26.

Tian, Y., Lei, L. and Minden, A. (2011). A key role for Pak4 in proliferation and differentiation of neural progenitor cells. *Dev. Biol.* **353**, 206-216.

Truman, J. W. and Bate, M. (1988). Spatial and temporal patterns of neurogenesis in the central nervous system of Drosophila melanogaster. *Dev. Biol.* **125**, 145-157.

Tzur, A., Kafri, R., LeBleu, V. S., Lahav, G. and Kirschner, M. W. (2009). Cell growth and size homeostasis in proliferating animal cells. *Science* **325**, 167-171.

Urbach, R. and Technau, G. M. (2004). Neuroblast formation and patterning during early brain development in Drosophila. *Bioessays* **26**, 739-751.

Urbach, R., Schnabel, R. and Technau, G. M. (2003). The pattern of neuroblast formation, mitotic domains and proneural gene expression during early brain development in Drosophila. *Development* **130**, 3589-3606.

Wells, C. M. and Jones, G. E. (2010). The emerging importance of group II PAKs. *Biochem. J.* **425**, 465-473.

Wu, P. S., Egger, B. and Brand, A. H. (2008). Asymmetric stem cell division: lessons from Drosophila. *Semin. Cell Dev. Biol.* **19**, 283-293.

Yu, F., Cai, Y., Kaushik, R., Yang, X. and Chia, W. (2003). Distinct roles of Galphai and Gbeta13F subunits of the heterotrimeric G protein complex in the mediation of Drosophila neuroblast asymmetric divisions. *J. Cell Biol.* **162**, 623-633.

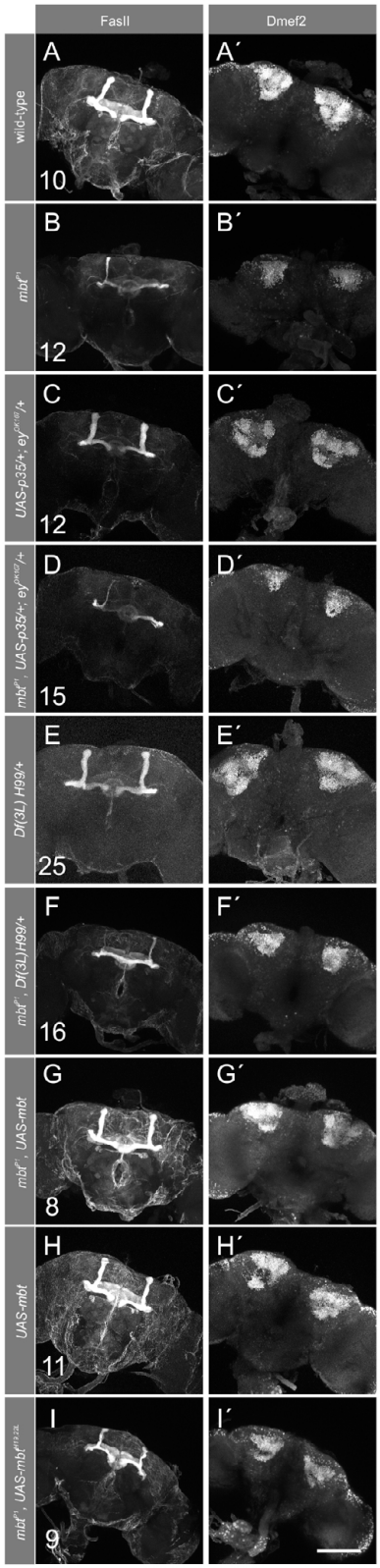

Fig. S1. Analysis of the adult mushroom body phenotype. Projections of confocal images of adult brains at the level of the lobe system (labeled with FasII) and the Kenyon cell layer (labeled with Dmef2) are shown. (**A-B′**) The lobe system and the Kenyon cell cluster are both severely reduced in mbt^{P1} brains compared with the wild type. Frequently, α/β-lobes are completely missing. (**C**,**C′**) Expression of *UAS-p35* in a wild-type background (using ey^{OK107} that post-embryonically drives expression in Kenyon cells and not in MBNBs) does not interfere with the adult MB structure. (**D**,**D′**) Expression of *UAS-p35* in mbt^{P1} animals does not rescue the mbt^{P1} phenotype. (**E-F′**) *Df(3L)H99* does not change adult MB structure in the wild type. No rescue of MB size is observed with *Df(3L) H99* in mbt^{P1} background. (**G**,**G′**) Neuroblast-specific expression of an *mbt*-transgene in mbt^{P1} background with *worniu-GAL4* rescues the MB size to wild-type level. (**H**,**H′**) No influence on MB structure was observed upon expression of the *mbt* transgene in wild-type background. (**I**,**I′**) Expression of $mbt^{H19,22L}$ resulted in partial rescue of MB size. The numbers of brains analyzed are indicated in the images. Scale bar: 100 µm.